Axial translation of a rigid disc inclusion embedded in a penny-shaped crack in a transversely isotropic solid

S. M. Dehghan Manshadi[a], A. Khojasteh[b,*], M. Rahimian[a]

[a]School of Civil Engineering, College of Engineering, University of Tehran, P.O. Box 11155-4563, Tehran, Iran.
[b]School of Engineering Science, College of Engineering, University of Tehran, P.O. Box 11155-4563, Tehran, Iran.

Abstract

In this paper, an analytical solution for the axisymmetric interaction of a rigid disc inclusion embedded in bonded contact with the surfaces of a penny-shaped crack and a transversely isotropic medium is investigated. By using a method of potential functions and treating dual and triple integral equations, the mixed boundary value problem is written in the form of two coupled integral equations, which are amenable to numerical treatments. The axial stiffness of the inclusion and the shearing stress intensity factor at the tip of the penny-shaped crack for different degrees of material anisotropy are illustrated graphically. Useful limiting cases such as a rigid disc inclusion in an uncracked medium and in a completely cracked solid are recovered.

Keywords: Penny-shaped crack, Rigid disc, Transversely isotropic, Axial stiffness, Stress intensity factor, Integral equation

1. Introduction

The category of problems that examines the mechanical behavior of contact regions constitutes an important branch of applied mechanics with extensive engineering applications [1]. Nowadays composites play a very important role in geomechanics engineering. It is common knowledge that all existing structural materials contain different inter- and intra-component defects (cracks, delaminations, etc.) [2]. Analysis of interaction between cracks and inclusions has important applications to the study of micro-mechanics of multiphase materials and to the examination of anchoring devices embedded in geological media [3].

The distribution of stress produced in the interior of an elastic solid by the opening of an internal crack under the action of pressure applied to its surface was considered by Sneddon [4] (see also [5, 6]). Sneddon and Lowengrub [7] and Kassir and Sih [8] by considering various boundary conditions of the crack surfaces obtained associated

*Corresponding author. Tel.: +982161112232; Mobile: +98912 695 6717; Fax: +98 21 88078263
Email addresses: m.manshadi70@ut.ac.ir (S. M. Dehghan Manshadi), akhojasteh@ut.ac.ir (A. Khojasteh), rahimian@ut.ac.ir (M. Rahimian)

stress intensity factors. Sih [9] considered the influence of plate thickness on the stress distribution around the crack. The axially symmetric elastostatic problem for a layer bonded to a half-space with different material properties was investigated by Erdogan and Arin [10]. Dynamic stress intensity factor for a penny-shaped crack embedded in an infinite elastic medium under time harmonic torsional body forces was investigated by Rahman [11]. The study of an infinite domain containing a penny-shaped crack which is loaded axially by a rigid disc inclusion in an isotropic elastic medium was performed by Selvadurai et al. [12]. Analysis of the problem pertinent to the complete indention of a single face of a penny-shaped crack by a rigid smooth inclusion was performed by Selvadurai [3]. The problem of examining the axial tensile loading of a rigid circular disc which is bonded to the surface of a half-space weakened by a penny-shaped crack was considered by Selvadurai [1]. Selvadurai [13] studied the axial loading of an annular crack by a rigid disc inclusion and presented the shearing stress intensity factor and the axial stiffness of the inclusion for different ratios of the inner and outer radius of the annular crack. Vrbik et al. [14] studied the symmetric indention of a penny-shaped crack by a smoothly embedded rigid circular disc inclusion in a thick layer.

Recently, separation of dissimilar piezoelectric half-spaces by a rigid disc inclusion has been discussed by Eskandari et al. [15]. Shodja et al. [16] analyzed the interaction of the annular and penny-shaped crack in an infinite piezoelectric medium (see also [17]). The study of indentation of an elliptic crack by a rigid elliptic inclusion in the anti-plane shear mode was performed by Singh et al. [18]. Eskandari-Ghadi et al. [19] presented a mathematical formulation for the analysis of a transversely isotropic half-space containing a disc-shaped crack buried at an arbitrary depth. Fabrikant [20] considered a transversely isotropic body weakened in the plane perpendicular to the planes of isotropy of the transversely isotropic body (see also [21–23]). The influence of a capillary bridge or a liquid droplet on the crack opening and stress intensity factor of a penny-shaped crack under a far-field tensile stress is investigated by Yang and Zhao [24]. Shahmohamadi et al. [25] studied the axial interaction of a rigid disc with a penny-shaped crack in a transversely isotropic full-space. Moreover, the plane problem of interaction between a thin rigid inclusion and a finite crack was studied by Antipov and Mkhitaryan [26]. Amiri-Hezaveh et al. [27] examined the dynamic indention of a rigid circular plate embedded in a non-homogeneous transversely isotropic full-space. Eskandari-Ghadi et al. [28] presented an analytical solution for a two-layer transversely isotropic half-space containing a penny-shaped crack located at the interface of layers.

In this paper, the main objective is to investigate the interaction of a rigid disc in bonded contact with the surfaces of a penny-shaped crack and an infinite transversely isotropic medium. By virtue of appropriate displacement-potential functions and Hankel and Abel transforms, the solution of the problem is reduced to two coupled Fredholm integral equations, which are amenable to numerical treatments. The axial stiffness of the inclusion and the mode II stress intensity factor at the tip of the crack are obtained for several types of hypothetical transversely isotropic materials.

From a practical viewpoint, in geomechanical applications, the rigid disc-shaped inclusion represents the behavior of an earth or rock anchor which is created by the hydraulic fracture of the earth or rock mass. The inclusion represents the resinous or cementing material which is used to transfer anchoring loads to the geological medium [29].

2. Statement of the problem and the governing equations

Consider a rigid circular disc inclusion of radius a surrounded by a penny-shaped crack of radius b in an infinite transversely isotropic medium while the disc is in perfect contact with the surfaces of the crack (see Figure 1). The disc is subjected to a central force T which induces a rigid-body displacement δ in the z direction. Because of symmetry, it suffices to limit attention to one half-space ($0 \le z < \infty$). The mixed boundary conditions of the problem under consideration in terms of the displacement vector $\boldsymbol{u}$ and the Cauchy stress tensor $\boldsymbol{\sigma}$ are as follows

$$u_z(r,0) = \delta, \qquad 0 \le r \le a \tag{1}$$

$$u_r(r,0) = 0, \qquad 0 \le r \le a, \qquad b \le r < \infty \tag{2}$$

$$\sigma_{zz}(r,0) = 0, \qquad a < r < \infty \tag{3}$$

$$\sigma_{rz}(r,0) = 0, \qquad a < r < b \tag{4}$$

Figure 1

For axisymmtric problems, the equilibrium equations of the static motion for a homogeneous transversely isotropic elastic solid in terms of displacement and in the absence of the body forces can be expressed as [30]

$$\begin{aligned} &c_{11}\left(\frac{\partial^2 u_r}{\partial r^2} + \frac{1}{r}\frac{\partial u_r}{\partial r} - \frac{u_r}{r^2}\right) + c_{44}\frac{\partial^2 u_r}{\partial z^2} + (c_{13}+c_{44})\frac{\partial^2 u_r}{\partial r \partial z} = 0 \\ &c_{44}\left(\frac{\partial^2 u_z}{\partial r^2} + \frac{1}{r}\frac{\partial u_z}{\partial r}\right) + c_{33}\frac{\partial^2 u_z}{\partial z^2} + (c_{13}+c_{44})\left(\frac{\partial^2 u_r}{\partial r \partial z} + \frac{1}{r}\frac{\partial u_r}{\partial z}\right) = 0 \end{aligned} \tag{5}$$

where u_r and u_z are the displacement components in the r and z directions, respectively; and c_{ij} are the elasticity constants of the solid. The displacement and stress fields for a semi-infinite transversely isotropic medium ($0 \le z < \infty$)

are as below [31]

$$
\begin{aligned}
u_z(r,z) &= \int_0^\infty -\xi^3 \left[A'(\xi)\left(1+\alpha_1 - s_1^2\alpha_2\right)\mathrm{e}^{-\xi s_1 z} + B'(\xi)\left(1+\alpha_1 - s_2^2\alpha_2\right)\mathrm{e}^{-\xi s_2 z}\right] J_0(\xi r)\,\mathrm{d}\xi \\
u_r(r,z) &= \int_0^\infty -\xi^3\alpha_3 \left[A'(\xi)s_1\mathrm{e}^{-\xi s_1 z} + B'(\xi)s_2\mathrm{e}^{-\xi s_2 z}\right] J_1(\xi r)\,\mathrm{d}\xi \\
\sigma_{zz}(r,z) &= \int_0^\infty -\xi^4(A'(\xi)s_1\mathrm{e}^{-\xi s_1 z} + B'(\xi)s_2\mathrm{e}^{-\xi s_2 z})\left[c_{33}\alpha_2\left(s_1^2+s_2^2\right) + (c_{13}\alpha_3 - c_{33}\left(1+\alpha_1\right))\right] J_0(\xi r)\,\mathrm{d}\xi \\
\sigma_{rz}(r,z) &= \int_0^\infty \xi^4 \mathrm{c}_{44}\left[A'\left(\xi\right)\left(1+\alpha_1+s_1^2\left(\alpha_3-\alpha_2\right)\right)\mathrm{e}^{-\xi s_1 z} + B'(\xi)\left(1+\alpha_1+s_2^2\left(\alpha_3-\alpha_2\right)\right)\mathrm{e}^{-\xi s_2 z}\right] J_1(\xi r)\,\mathrm{d}\xi
\end{aligned}
\tag{6}
$$

where $A'(\xi)$ and $B'(\xi)$ are unknown functions and

$$
\alpha_1 = \frac{c_{12}+c_{66}}{c_{66}}, \qquad \alpha_2 = \frac{c_{44}}{c_{66}}, \qquad \alpha_3 = \frac{c_{13}+c_{44}}{c_{66}} \tag{7}
$$

Here s_1 and s_2 are the roots of following equation, which in view of the positive-definiteness of the strain energy are not zero or pure imaginary numbers [30]

$$
c_{33}c_{44}s^4 - [c_{13}^2 + 2c_{13}c_{44} - c_{11}c_{33}]s^2 + c_{11}c_{44} = 0 \tag{8}
$$

Introducing the substitutions

$$
[A(\xi); B(\xi)] = \frac{1}{\xi^2}[A'(\xi); B'(\xi)] \tag{9}
$$

and using the relation (6), the boundary conditions (1)-(4) can be reduced to the following system of integral equations

$$
\int_0^\infty M(\xi)J_0(\xi r)\,\mathrm{d}\xi = \delta, \qquad 0 \le r \le a \tag{10}
$$

$$
\int_0^\infty N(\xi)J_1(\xi r)\,\mathrm{d}\xi = \gamma_1 \int_0^\infty M(\xi)J_1(\xi r)\,\mathrm{d}\xi, \qquad 0 \le r \le a, \qquad b \le r < \infty \tag{11}
$$

$$
\int_0^\infty \xi M(\xi)J_0(\xi r)\,\mathrm{d}\xi = \gamma_2 \int_0^\infty \xi N(\xi)J_0(\xi r)\,\mathrm{d}\xi, \qquad a < r < \infty \tag{12}
$$

$$
\int_0^\infty \xi N(\xi)J_1(\xi r)\,\mathrm{d}\xi = 0, \qquad a < r < b \tag{13}
$$

where γ_k $(k = 1,2)$ and the functions $M(\xi)$ and $N(\xi)$ are mentioned in Appendix A.

2.1. *Dual integral equations*

Making use of Eqs. (10) and (12) the following system of dual integral equations are obtained

$$\int_0^\infty M(\xi)J_0(\xi r)\,\mathrm{d}\xi = \delta, \qquad 0 \le r \le a \tag{14}$$

$$\int_0^\infty \xi M(\xi)J_0(\xi r)\,\mathrm{d}\xi = \gamma_2 \int_0^\infty \xi N(\xi)J_0(\xi r)\,\mathrm{d}\xi, \qquad a < r < \infty \tag{15}$$

The integral Eqs. (14) and (15) yield the following

$$M(\xi) = \frac{2}{\pi}\left[\frac{\delta \sin(\xi a)}{\xi} + \int_a^\infty F(u)\cos(\xi u)\,\mathrm{d}u\right] \tag{16}$$

where

$$F(t) = \gamma_2 \int_0^\infty N(\xi)\cos(\xi t)\,\mathrm{d}\xi \tag{17}$$

2.2. *Triple integral equations*

Making use of Eqs. (11) and (13) the following system of triple integral equations are obtained

$$\int_0^\infty N(\xi)J_1(\xi r)\,\mathrm{d}\xi = \gamma_1 \int_0^\infty M(\xi)J_1(\xi r)\,\mathrm{d}\xi, \qquad 0 \le r \le a \tag{18}$$

$$\int_0^\infty \xi N(\xi)J_1(\xi r)\,\mathrm{d}\xi = 0, \qquad a < r < b \tag{19}$$

$$\int_0^\infty N(\xi)J_1(\xi r)\,\mathrm{d}\xi = \gamma_1 \int_0^\infty M(\xi)J_1(\xi r)\,\mathrm{d}\xi, \qquad b \le r < \infty \tag{20}$$

Taking the following assumption

$$\int_0^\infty \xi N(\xi)J_1(\xi r)\,\mathrm{d}\xi = \begin{cases} f_1(r), & 0 < r < a \\ 0, & a < r < b \\ f_2(r), & b < r < \infty \end{cases} \tag{21}$$

By employing the inverse Hankel integral transform to (21), we obtain the relation

$$N(\xi) = \int_0^a r f_1(r)J_1(\xi r)\,\mathrm{d}r + \int_b^\infty r f_2(r)J_1(\xi r)\,\mathrm{d}r \tag{22}$$

Inserting (22) into (11), we have

$$I_1(r) + I_2(r) = g(r), \qquad 0 < r < a \tag{23}$$

$$I_1(r) + I_2(r) = g(r), \qquad b < r < \infty \tag{24}$$

where

$$I_j(r) = \int \lambda f_j(\lambda) L(r,\lambda)\,\mathrm{d}\lambda, \qquad (j = 1,2) \tag{25}$$

$$L(r,\lambda) = \int_0^\infty J_1(\xi r) J_1(\xi\lambda)\,\mathrm{d}\xi \tag{26}$$

$$g(r) = \gamma_1 \int_0^\infty M(\xi) J_1(\xi r)\,\mathrm{d}\xi \tag{27}$$

and the limits of integration in (25) can occupy the ranges $(0,a)$ and (b,∞) depending upon the value of j.

Using the procedure presented in the paper [32], Eqs. (23) and (24) can be rewritten as

$$\int_0^r \frac{F_1(s)\,\mathrm{d}s}{(r^2-s^2)^{1/2}} = -r^2 \int_b^\infty \frac{F_2(s)\,\mathrm{d}s}{s^2(s^2-r^2)^{1/2}} + \frac{\pi r}{2} g(r), \qquad 0 < r < a \tag{28}$$

$$\int_r^\infty \frac{F_2(s)\,\mathrm{d}s}{s^2(s^2-r^2)^{1/2}} = -\frac{1}{r^2} \int_0^a \frac{F_1(s)\,\mathrm{d}s}{(r^2-s^2)^{1/2}} + \frac{\pi}{2r} g(r), \qquad b < r < \infty \tag{29}$$

where

$$F_1(s) = s^2 \int_s^a \frac{f_1(u)\,\mathrm{d}u}{(u^2-s^2)^{1/2}} \tag{30}$$

$$F_2(s) = \int_b^s \frac{u^2 f_2(u)\,\mathrm{d}u}{(s^2-u^2)^{1/2}} \tag{31}$$

Eqs. (28) and (29) are the Abel type integral equations, which their solutions are as follows

$$F_1(s) = -\frac{2}{\pi} \int_b^\infty \left[-\frac{s^2}{u(s^2-u^2)} + \frac{s}{2u^2} \ln\left|\frac{s+u}{s-u}\right| \right] F_2(u)\,\mathrm{d}u + \frac{\mathrm{d}}{\mathrm{d}s} \int_0^s \frac{r^2 g(r)\,\mathrm{d}r}{(s^2-r^2)^{1/2}}, \qquad 0 < s < a \tag{32}$$

$$F_2(s) = -s^2 \frac{\mathrm{d}}{\mathrm{d}s} \int_s^\infty \frac{g(r)\,\mathrm{d}r}{(r^2-s^2)^{1/2}} - \frac{2}{\pi} \int_0^a \left[\frac{s}{s^2-u^2} + \frac{1}{2u} \ln\left|\frac{s+u}{s-u}\right| \right] F_1(u)\,\mathrm{d}u, \qquad b < s < \infty \tag{33}$$

Using the following relations

$$\frac{\mathrm{d}}{\mathrm{d}s}\int_0^s \frac{r^2 J_1(\xi r)\mathrm{d}r}{\sqrt{s^2-r^2}} = s\sin(\xi s) \tag{34}$$

$$\frac{\mathrm{d}}{\mathrm{d}s}\int_s^\infty \frac{J_1(\xi r)\mathrm{d}r}{\sqrt{r^2-s^2}} = \frac{\cos(\xi s)}{s} - \frac{\sin(\xi s)}{\xi s^2} \tag{35}$$

and Eq. (27), we have

$$\frac{\mathrm{d}}{\mathrm{d}s}\int_0^s \frac{r^2 g(r)\,\mathrm{d}r}{(s^2-r^2)^{1/2}} = \gamma_1 s\int_0^\infty M(\xi)\sin(\xi s)\,\mathrm{d}\xi, \qquad 0<s<a \tag{36}$$

$$s^2\frac{\mathrm{d}}{\mathrm{d}s}\int_s^\infty \frac{g(r)\,\mathrm{d}r}{(r^2-s^2)^{1/2}} = \gamma_1\int_0^\infty \frac{1}{\xi}[\xi s\cos(\xi s)-\sin(\xi s)]M(\xi)\,\mathrm{d}\xi, \qquad b<s<\infty \tag{37}$$

Insertion of Eqs. (36) and (37) into Eqs. (32) and (33), yields the following coupled Fredholm integral equations

$$\begin{aligned} &F_1(s) - \frac{2}{\pi^2}\gamma_1\gamma_2\int_0^a \frac{sF_1(u)}{u(u^2-s^2)}\left[u\ln\left|\frac{a-s}{a+s}\right| - s\ln\left|\frac{a-u}{a+u}\right|\right]\mathrm{d}u \\ &+\frac{2}{\pi}\int_b^\infty\left[-\frac{s^2}{u(s^2-u^2)}+\frac{s}{2u^2}\ln\left|\frac{s+u}{s-u}\right|\right]F_2(u)\,\mathrm{d}u \\ &+\frac{2}{\pi}\gamma_1\gamma_2\int_b^\infty\left[\frac{s}{2u^2}\ln\left|\frac{(u-s)(a+s)}{(u+s)(a-s)}\right| - \frac{s^2}{u(u^2-s^2)}\right]F_2(u)\,\mathrm{d}u = \frac{\gamma_1\delta}{\pi}s\ln\left|\frac{s+a}{s-a}\right|, \qquad 0<s<a \end{aligned} \tag{38}$$

$$\begin{aligned} &(1-\gamma_1\gamma_2)\,F_2(s) + \frac{2}{\pi}\int_0^a\left[\frac{s}{s^2-u^2}+\frac{1}{2u}\ln\left|\frac{s+u}{s-u}\right|\right]F_1(u)\,\mathrm{d}u - \frac{2}{\pi}\gamma_1\gamma_2\int_0^a\frac{sF_1(u)}{s^2-u^2}\,\mathrm{d}u \\ &+\gamma_1\gamma_2 a\int_c^\infty\frac{F_2(u)}{u^2}\,\mathrm{d}u + \frac{\gamma_1\gamma_2}{\pi}\int_0^a\frac{F_1(u)}{u}\ln\left|\frac{(s-u)(a+u)}{(s+u)(a-u)}\right|\mathrm{d}u = \gamma_1 a\delta, \qquad b<s<\infty \end{aligned} \tag{39}$$

We can rewrite (38) and (39) in the general forms

$$\phi_1(s) + \int_0^a \phi_1(u)K_{11}(u,s)\,\mathrm{d}u + \int_b^\infty \phi_2(u)K_{12}(u,s)\,\mathrm{d}u = L_1(s)\delta, \qquad 0<s<a \tag{40}$$

$$R\phi_2(s) + \int_0^a \phi_1(u)K_{21}(u,s)\,\mathrm{d}u + \int_b^\infty \phi_2(u)K_{22}(u,s)\,\mathrm{d}u = L_2(s)\delta, \qquad b<s<\infty \tag{41}$$

where we have assumed that $F_1(s)$ and $F_2(s)$ admit representations of the form

$$[F_1(u);F_2(u)] = \frac{\gamma_1 u}{\pi}[\phi_1(u);\phi_2(u)] \tag{42}$$

and the kernel functions K_{ij} $(i,j=1,2)$ are expressed as

$$
\begin{aligned}
K_{11}(u,s) &= \frac{\eta_1}{u^2-s^2}\left(u\ln\left|\frac{a-s}{a+s}\right| - s\ln\left|\frac{a-u}{a+u}\right|\right)\\
K_{22}(u,s) &= \eta_2\frac{a}{su}\\
K_{12}(u,s) &= \eta_3\left(-\frac{s}{s^2-u^2}+\frac{1}{2u}\ln\left|\frac{s+u}{s-u}\right|\right)+\eta_4\frac{1}{2u}\ln\left|\frac{a+s}{a-s}\right|\\
K_{21}(u,s) &= \eta_3\left(-\frac{u}{u^2-s^2}+\frac{1}{2s}\ln\left|\frac{u+s}{u-s}\right|\right)+\eta_4\frac{1}{2s}\ln\left|\frac{a+u}{a-u}\right|
\end{aligned}
\tag{43}
$$

The constants R and η_k $(k=1,...,4)$ are given by

$$
\begin{aligned}
&R = 1-\gamma_1\gamma_2\\
&\eta_1 = -\frac{2}{\pi^2}\gamma_1\gamma_2, \qquad \eta_2 = \gamma_1\gamma_2\\
&\eta_3 = \frac{2}{\pi}(1-\gamma_1\gamma_2), \quad \eta_4 = \frac{2}{\pi}\gamma_1\gamma_2
\end{aligned}
\tag{44}
$$

and the functions $L_1(s)$ and $L_2(s)$ are defined by

$$
L_1(s) = \ln\left|\frac{s+a}{s-a}\right|, \quad L_2(s) = \frac{\pi a}{s}
\tag{45}
$$

3. Contact-load distribution and axial stiffness

A practical interest result is the load-displacement relationship. The resultant force T acting on the disc is calculated by

$$
T = 2\int_0^{2\pi}\int_0^a r\sigma_{zz}(r,0)\,\mathrm{d}r\mathrm{d}\theta
\tag{46}
$$

where the axial stress, σ_{zz}, in the inclusion region is given by

$$
\sigma_{zz}(r,0) = \int_0^\infty \xi M(\xi)J_0(\xi r)\,\mathrm{d}\xi - \gamma_2\int_0^\infty \xi N(\xi)J_0(\xi r)\,\mathrm{d}\xi, \qquad 0<r<a
\tag{47}
$$

Employing the identities $M(\xi)$ and $N(\xi)$ as defined in (16) and (22), Eq. (46) simplifies to

$$
T = 8a\eta_4 + \frac{8\gamma_1\eta_3}{\pi^2}\left[\int_0^a \phi_1(u)\ln\left|\frac{a+u}{a-u}\right|\mathrm{d}u + \pi a\int_b^\infty \frac{\phi_2(u)}{u}\mathrm{d}u\right]
\tag{48}
$$

4. Stress intensity factor at the crack tip

A quantity of physical interest, which is applicable in fracture mechanics, is the stress intensity factor. Due to asymmetric deformation about $z = 0$, the only non-zero stress component is σ_{rz}. The mode II stress intensity factor is defined by

$$K_{II}^{b} = \lim_{r \to b^{+}} [2(r - b)]^{1/2} \sigma_{rz}(r, 0) \tag{49}$$

where

$$\sigma_{rz}(r, 0) = \int_{0}^{\infty} \xi N(\xi) J_1(\xi r)\, \mathrm{d}\xi, \qquad r > b \tag{50}$$

Utilizing the relation (21), we find that

$$\sigma_{rz}(r, 0) = \frac{2F_2(b)}{\pi r (r^2 - b^2)^{1/2}} + \frac{2}{\pi r} \int_{b}^{r} \frac{F_2'(s)\mathrm{d}s}{(r^2 - s^2)^{1/2}}, \qquad r > b \tag{51}$$

Inserting Eq. (42) and Eq. (51) into (49), the mode II stress intensity factor can be expressed as

$$K_{II}^{b} = \frac{2\gamma_1 \phi_2(b)}{\pi^2 \sqrt{b}} \tag{52}$$

5. Special cases

Before proceeding to the numerical solution of the general problem, it is relevant to examine some limiting cases which their solutions are available. Here, five special cases are inferred: (i) intact medium (ii) completely cracked solid (iii) direct loading of a penny-shaped crack (iv) $s_2 \to s_1$ (v) effect of incompressible materials

5.1. Inclusion in an uncracked elastic solid full-space

The force T required to achieve the disc displacement δ in the z direction is equal to (see Figure 2a)

$$T = \frac{8c_{44}c_{33}a\delta(s_1 + s_2)}{c_{44} + \sqrt{c_{11}c_{33}}} \tag{53}$$

for a transversely isotropic medium [33] and for an isotropic medium simplifies to [34]

$$T = \frac{32Ga\delta(1 - \nu)}{3 - 4\nu} \tag{54}$$

where G and ν are the elastic shear modulus and Poisson's ratio for an isotropic medium, respectively.

5.2. *Disc inclusion embedded between two half-space regions*

Taking the limit $a/b \to 0$ (with $a \neq 0$), the problem turns into the disc inclusion which is embedded between two identical half-space regions (see Figure 2b). In this case, the total force is

$$T = \frac{2a\theta\delta}{H\tanh(\pi\theta)} \tag{55}$$

where H and θ are mentioned in Appendix B. This relation is for a transversely isotropic medium as reported by Fabrikant [35] and for an isotropic medium simplifies to [36]

$$T = \frac{8Ga\delta\ln(3-4\nu)}{1-2\nu} \tag{56}$$

5.3. *Direct loading of a penny-shaped crack*

The exact mode II stress intensity factor of a penny-shaped crack in an infinite transversely isotropic medium due to a axial point force parallel to the z-axis applied at the center of the crack obtains as follows [37]

$$K_{II}^{b} = \frac{T}{2\pi b^{3/2}}\left(\frac{m_1 s_1}{m_1-1} + \frac{m_2 s_2}{m_2-1}\right) \tag{57}$$

where m_k $(k = 1,2)$ are defined in Appendix B, which for the isotropic case simplifies to [8]

$$K_{II}^{b} = \frac{T(1-2\nu)}{8\pi(1-\nu)b^{3/2}} \tag{58}$$

In this study, as $a \to 0$ (see Figure 2c), which means the inclusion disappears, the parameter T in (57) and (58) can be obtained from (55) and (56), respectively.

Figure 2a

Figure 2b

Figure 2c

5.4. s_1 *and* s_2 *become equal*

By substituting $s_1 = s_2$ into (6), terms with forms of $0/0$ will be encountered. This occurs in transversely isotropic materials when $\sqrt{c_{11}c_{33}} - c_{13} - 2c_{44} = 0$. In this case, one can obtain $s_1 = s_2 = (c_{11}/c_{33})^{1/4}$. Therefore, in order to obtain displacement and stress potential relations of the case of $s_1 = s_2$, it is needed to take the limits by setting $s_2 \to s_1$. The results are presented in Appendix C.

5.5. *Material incompressibility effect in an isotropic medium*

In the limiting case of material incompressibility ($\nu = 0.5$), Eqs. (54) and (56) reduce to the same result as

$$T = 16Ga\delta \tag{59}$$

From the above relation, it is evident that in the incompressible elastic materials the extent of cracking, increase in the value of b, at the plane containing the rigid inclusion, has no effect on the axial stiffness of the inclusion (see [38]).

6. The numerical evaluation of the governing integral equations

The simultaneous coupled Fredholm integral equations of the second kind (40) and (41) governing the axisymmetric interaction of a penny-shaped crack and a rigid disc inclusion are not amenable to solution in an exact form. A variety of techniques have been proposed for the numerical solution of coupled systems of Fredholm integral equations of the general type described by Baker [39] and Atkinson [40].

To solve these coupled integral equations numerically, the integration intervals $(0, a)$ and (b, ∞) are divided to N_1, N_2 segments, respectively, end points of the segments can be expressed as

$$\begin{aligned} x_i &= (2i-1)h_1 \qquad \text{with } i = 1, 2, \dots, N_1 \\ t_i &= t_{i-1} + \alpha(t_{i-1} + t_{i-2}) \qquad \text{with } i = 3, 4, \dots, N_2 + 1 \end{aligned} \tag{60}$$

where $h_1 = a/2N_1$, $t_1 = b$, $t_2 = b + a/N_1$ and α is a constant of proportionality such that the interval (b, ∞) is approximated in the numerical scheme. For the treatment of coupled integral equations (40) and (41), according to standard quadrature method, the integral equations can be written in the discretized form as

$$\begin{bmatrix} D_1 & D_2 \\ D_3 & D_4 \end{bmatrix} \begin{Bmatrix} \phi_1(s) \\ \phi_2(s) \end{Bmatrix} = \begin{Bmatrix} L_1(s) \\ L_2(s) \end{Bmatrix} \tag{61}$$

where

$$D_1 = \delta_{ij} + \sum_{i=1}^{N_1}\sum_{j=1}^{N_1} \frac{w_j \eta_1}{u_j^2 - s_i^2}\left[u_j \ln\left|\frac{a-s_i}{a+s_i}\right| - s_i \ln\left|\frac{a-u_j}{a+u_j}\right|\right], \qquad i \neq j \tag{62}$$

$$D_1 = \delta_{ii} + \sum_{i=1}^{N_1} \frac{w_i \eta_1}{2s_i}\left[\frac{2as_i}{a^2 - s_i^2} + \ln\left|\frac{a-s_i}{a+s_i}\right|\right], \qquad i = j \tag{63}$$

$$D_2 = \sum_{i=1}^{N_1}\sum_{j=1}^{N_2} w_j \eta_3 \left[-\frac{s_i}{s_i^2 - u_j^2} + \frac{1}{2u_j}\ln\left|\frac{s_i+u_j}{s_i-u_j}\right|\right] + \eta_4 \frac{1}{2u_j}\ln\left|\frac{a+s_i}{a-s_i}\right| \tag{64}$$

$$D_3 = \sum_{i=1}^{N_2}\sum_{j=1}^{N_1} w_j \eta_3 \left[-\frac{u_j}{u_j^2 - s_i^2} + \frac{1}{2s_i}\ln\left|\frac{u_j+s_i}{u_j-s_i}\right|\right] + \eta_4 \frac{1}{2s_i}\ln\left|\frac{a+u_j}{a-u_j}\right| \tag{65}$$

$$D_4 = R\delta_{ij} + \sum_{i=1}^{N_2}\sum_{j=1}^{N_2} w_j \eta_2 \frac{a}{s_i u_j} \tag{66}$$

where δ_{ij} is the Kronecker delta and w_j, the weight function, is

$$w_j = \begin{cases} \dfrac{a}{N_1}, & 0 < r < a \\ t_{i+1} - t_i, & b < r < \infty \end{cases} \tag{67}$$

The total load acting on the inclusion from Eq. (48) is

$$\frac{T}{\delta} = 8a\eta_4 + \frac{8\gamma_1\eta_3}{\pi^2}\left[\sum_{i=1}^{N_1} w_i \phi_1(u_i) \ln\left|\frac{a+u_i}{a-u_i}\right| + \pi a \sum_{i=1}^{N_2} w_i \frac{\phi_2(u_i)}{u_i}\right] \tag{68}$$

It can be written in terms of axial stiffness which is defined as

$$\bar{T} = \frac{T}{c_{44} a \delta} \tag{69}$$

The stress intensity factor, defined by (52), can be expressed in the form

$$K_{II}^b = \frac{2\delta\gamma_1\phi_2(b)}{\pi^2\sqrt{b}} \tag{70}$$

The normalized stress intensity factor can take the form

$$\bar{K}_{II}^b = \frac{K_{\mathrm{II}}^b b^{3/2}}{c_{44} a \delta} \tag{71}$$

7. Numerical results and discussion

To confirm the validity of the present solution and evaluate the effects of anisotropic materials on the results, several synthetic types of isotropic (material 1) and transversely isotropic materials (materials 2-9) are selected. The material properties are given in Table 1, where E and E' are the Young's modules in the plane of isotropy and perpendicular to it, respectively; ν' is Poisson's ratio that characterizes the effect of horizontal strain on the complementary vertical strain; ν is the Poisson's ratio which characterizes the effect of vertical strain on the horizontal one; and G' stands for the shear modulus for the plane normal to the plane of isotropy. Regarding the positive-definiteness of strain energy, the following constraints for material constants c_{ij} have been checked (for example, see [41])

$$c_{11} > |c_{12}|, \qquad (c_{11} + c_{12})c_{33} > 2c_{13}^2, \qquad c_{44} > 0 \tag{72}$$

Table 1

Figure 3a

Figure 3b

Figure 3c

Axial stiffness as a function of the inclusion-crack aspect ratio is plotted in Figure 3. The influence of E'/E ratio is shown in Figure 3a, which presents that an increase in E'/E leads to a remarkable increase in the axial stiffness. From Figure 3b, one might notice that by decreasing G'/G the stiffness increases significantly. It can be concluded that the anisotropic parameters E' and G' have the main influence on the axial stiffness. In contrast, from Figure 3c, one can observe that the increase in E/E' and G/G', has little effect on the results. However, anisotropic parameters E and G are found to be of minor importance for the axial interaction of crack-inclusion.

Figure 4a

Figure 4b

Figure 4c

The results of the synthetic transversely isotropic materials for the normalized shearing stress intensity factor are presented in Figure 4. As indicated in Figure 4a, the larger the value of E'/E, the higher the response results in. Figure 4b shows the reduction in G'/G leads to the slightly increase in the mode II stress intensity factor. As shown in Figure 4c, changing the ratios of E/E' and G/G' has a significant influence on the σ_{rz} and K_{II}^b.

In the limiting $a \to b$, the normalized stress intensity factor decreases sharply, which is due to the oscillatory of the stress singularity. Selvadurai [12] has been shown that such oscillatory stress singularities have virtually no influence on the accuracy of the translational stiffness. In this study, $\bar{K}_{II}^{b}$ is depicted for the interval $(0, 0.9)$. Hilbert solution has been suggested to overcome this problem in the integral transform method.

8. Conclusions

The analytical treatment of the interaction crack-inclusion in a transversely isotropic full-space is revisited. By virtue of appropriate potential functions, the mixed boundary value problem is reduced to dual and triple integral equations. By employing suitable representations and Abel transforms, the results are expressed in terms of the solution of two coupled Fredholm integral equations, which are solved by using a numerical method. The available closed-form results in the literature such as the inclusion in an intact medium are recovered as the limiting cases of the current study. The axial stiffness of the inclusion and the shearing stress intensity factor at the tip of the crack are obtained for some synthetic transversely isotropic materials. The effects of material anisotropy on the results are also highlighted.

References

[1] Selvadurai, A.P.S. “Mechanics of a rigid circular disc bonded to a cracked elastic half-space,” *Int. J. Solids Struct.*, **39**(24), pp. 6035–6053 (2002).

[2] Menshykov, O.V., Menshykov, V.A. and Guz, I.A. “The contact problem for an open penny-shaped crack under normally incident tension-compression wave,” *Eng. Fract. Mech.*, **75**(5), pp. 1114–1126 (2008).

[3] Selvadurai, A.P.S. “A contact problem for a smooth rigid disc inclusion in a penny-shaped crack,” *Z. angew. Math. Phys. (ZAMP)*, **45**(1), pp. 166–173 (1994).

[4] Sneddon, I.N. “The distribution of stress in the neighbourhood of a crack in an elastic solid,” *Proc. Math. Phys. Eng. Sci.*, **187**, pp. 229–260 (1946).

[5] Collins, W. “Some axially symmetric stress distributions in elastic solids containing penny-shaped cracks. i. cracks in an infinite solid and a thick plate,” *Proc. Math. Phys. Eng. Sci.*, **266**, pp. 359–386 (1962).

[6] Sneddon, I.N. and Tweed, J. “The stress intensity factor for a penny-shaped crack in an elastic body under the action of symmetric body forces,” *Int. J. Fract. Mech.*, **3**(4), pp. 291–299 (1967).

[7] Sneddon, I.N. and Lowengrub, M. *Crack problems in the classical theory of elasticity*, 221pp (1969).

[8] Kassir, M. and Sih, G.C. *Three-dimensional crack problems: A new selection of crack solutions in three-dimensional elasticity*, Noordhoof International Publishing, Leyden (1975).

[9] Sih, G.C. "A review of the three-dimensional stress problem for a cracked plate," *Int. J. Fract. Mech.*, **7**(1), pp. 39–61 (1971).

[10] Erdogan, F. and Arin, K. "Penny-shaped interface crack between an elastic layer and a half space," *Int. J. Eng. Sci.*, **10**(2), pp. 115–125 (1972).

[11] Rahman, M. "A penny-shaped crack under time-harmonic torsional body forces," *Eng. Fract. Mech.*, **49**(4), pp. 599–610 (1994).

[12] Selvadurai, A.P.S., Singh, B.M. and Au, M. "Axial loading of a rigid disc inclusion with a debonded region," *Int. J. Solids Struct.*, **25**(7), pp. 783–795 (1989).

[13] Selvadurai, A.P.S. "On the axisymmetric loading of an annular crack by a disk inclusion," *J. Eng. Math.*, **46**(3-4), pp. 377–393 (2003).

[14] Vrbik, J., Singh, B.M., Rokne, J. and Dhaliwal, R.S. "On the expansion of a penny-shaped crack by a rigid circular disc inclusion in a thick plate," *Z. Angew. Math. Mech. (ZAMM)*, **84**(8), pp. 538–550 (2004).

[15] Eskandari, M., Moeini-Ardakani, S.S. and Shodja, H.M. "Axisymmetric contact of a rigid inclusion embedded at the interface of a piezoelectric bimaterial," *Quart. J. Mech. Appl. Math.*, **62**(3), pp. 281–295 (2009).

[16] Shodja, H.M., Moeini-Ardakani, S.S. and Eskandari, M. "Axisymmetric problem of energetically consistent interacting annular and penny-shaped cracks in piezoelectric materials," *J. Appl. Mech.*, **78**(2) pp. 021010-10 (2011).

[17] Eskandari, M., Moeini-Ardakani, S.S., and Shodja, H.M. "An energetically consistent annular crack in a piezoelectric medium," *Eng. Fract. Mech*, **77**(5), pp. 819–831 (2010).

[18] Singh, B.M., Rokne, J. and Dhaliwal, R.S. "Closed form solution for an annular elliptic crack around an elliptic rigid inclusion in an infinite solid," *J. Appl. Math. Mech. (ZAMM)*, **92**(11-12), pp. 882–887 (2012).

[19] Eskandari-Ghadi, M., Ardeshir-Behrestaghi, A. and Neya, B.N. "Mathematical analysis for an axissymmetric disc-shaped crack in transversely isotropic half-space," *Int. J. Mech. Sci.*, **68**, pp. 171–179 (2013).

[20] Fabrikant, V.I. "General flat crack located in the plane perpendicular to the planes of isotropy in transversely isotropic body," *Acta Mech.*, **226**(10), pp. 3289–3306 (2015).

[21] Fabrikant, V.I. “Non-traditional crack problem for transversely-isotropic body,” *Eur. J. Mech. A-Solid*, **30**(6), pp. 902–912 (2011).

[22] Fabrikant, V.I. “General flat crack arbitrarily located in the transversely-isotropic body,” *Theor. Appl. Fract. Mech.*, **82**, pp. 69–76 (2016).

[23] V. Fabrikant, “Relationship between contact and crack problems for generally anisotropic bodies,” *Int. J. Eng. Sci.*, **102**, pp. 27–35 (2016).

[24] Yang, F. and Zhao, Y.-P. “The effect of a capillary bridge on the crack opening of a penny crack,” *Soft matter*, **12**(5), pp. 1586–1592 (2016).

[25] Shahmohamadi, M., Khojasteh, A. and Rahimian, M. “Frictionless contact of a rigid disk with the face of a penny-shaped crack in a transversely isotropic solid,” *Int. J. Solids Struct.*, **106**, pp. 274-283 (2017).

[26] Antipov, Y.A. and Mkhitaryan, S.M. “A crack induced by a thin rigid inclusion partly debonded from the matrix,” *Quart. J. Mech. Appl. Math.*, **70**(2), pp. 153–85 (2017).

[27] Amiri-Hezaveh, A., Moghaddasi, H., Karimi, P., and Ostoja-Starzewski, M. “Dynamic interaction of plates in an inhomogeneous transversely isotropic space weakened by a crack,” *J. Appl. Math. Mech. (ZAMM)*, **97**, pp. 491–504 (2017).

[28] M. Eskandari-Ghadi, A. Ardeshir-Behrestaghi, and R. Y. Pak, “Bi-material transversely isotropic half-space containing penny-shaped crack under time-harmonic horizontal loads,” *Eng. Fract. Mech.*, **172**, pp. 152–180 (2017).

[29] Singh, B.M., Rokne, J. and Dhaliwal, R.S. “Thermal stresses in a two-dimensional infinite medium containing a rigid inclusion embedded in a line crack,” *Theor. Appl. Fract. Mech.*, **46**(2), pp. 148–155 (2006).

[30] Lekhnitskii, S. *Theory of an anisotropic elastic body*, vol. 525. Holden-Day, San Francisco (1963).

[31] Rahimian, M., Eskandari-Ghadi, M., Pak, R.Y.S. and Khojasteh, A. “Elastodynamic potential method for transversely isotropic solid,” *J. Eng. Mech.*, **133**(10), pp. 1134–1145 (2007).

[32] Cooke, J. “Triple integral equations,” *Quart. J. Mech. Appl. Math.*, **16**(2), pp. 193–203 (1963).

[33] Katebi, A.A., Khojasteh, A., Rahimian, M. and Pak, R.Y.S. “Axisymmetric interaction of a rigid disc with a transversely isotropic half-space,” *Int. J. Numer. Anal. Methods Geomech.*, **34**(12), pp. 1211–1236 (2010).

[34] Selvadurai, A.P.S. “Axial displacement of a rigid elliptical disc inclusion embedded in a transversely isotropic elastic solid,” *Mech. Res. Commun.*, **9**(1), pp. 39–45 (1982).

[35] Fabrikant, V.I. *Mixed boundary value problems of potential theory and their applications in engineering*, Kluwer Academic Publishers (1991).

[36] Mossakovskii, V. “The fundamental mixed problem of the theory of elasticity for a half-space with a circular line separating the boundary conditions,” *Prikl. Mat. Mekh.*, **18**, pp. 187–196 (1954).

[37] Fabrikant, V.I. *Applications of potential theory in mechanics: a selection of new results*, vol. 51, Kluwer Academic Publishers, Dordrecht; Boston (1989).

[38] Selvadurai, A.P.S. and Singh, B.M. “Axisymmetric problems for an externally cracked elastic solid-ii. effect of a penny-shaped inclusion,” *Int. J. Eng. Sci.*, **25**(11-12), pp. 1477–1490 (1987).

[39] Baker, C. *The Numerical Treatment of Integral Equations*, Clarendon Press (1977).

[40] Atkinson, K.E. *A survey of numerical methods for the solution of Fredholm integral equations of the second kind*, Soc. for Industrial and Applied Mathematics (1976).

[41] Payton, R.C. *Elastic wave propagation in transversely isotropic media*, Springer Science & Business Media (2012).

Appendix A

The parameters in Eqs. (10)-(13) are:

$$\gamma_1 = -\frac{C_2}{C_1} \tag{A.1}$$

$$\gamma_2 = -\frac{C_3}{C_4} \tag{A.2}$$

$$C_1 = -\frac{1+\alpha_1+s_1 s_2 \alpha_2}{c_{44}\left(s_1+s_2\right)\left(1+\alpha_1\right)} \tag{A.3}$$

$$C_2 = \frac{-1-\alpha_1+s_1 s_2\left(\alpha_3-\alpha_2\right)}{\left(s_1+s_2\right)\left(1+\alpha_1\right)} \tag{A.4}$$

$$C_3 = \frac{c_{33}\left(1+\alpha_1-s_1^2\alpha_2\right)\left(1+\alpha_1-s_2^2\alpha_2\right)-c_{13}\left(1+\alpha_1+s_1 s_2\alpha_2\right)\alpha_3}{c_{44}\left(s_1+s_2\right)\left(1+\alpha_1\right)\alpha_3} \tag{A.5}$$

$$C_4 = \frac{c_{33}\left(1+\alpha_1-s_1^2\alpha_2\right)\left(1+\alpha_1-s_2^2\alpha_2\right)-\left(c_{13}+c_{33}s_1 s_2\right)\left(1+\alpha_1+s_1 s_2\alpha_2\right)\alpha_3+c_{13}s_1 s_2\alpha_3^2}{\left(s_1+s_2\right)\left(1+\alpha_1\right)\alpha_3} \tag{A.6}$$

$$A(\xi) = \frac{\left(N\left(\xi\right)+M\left(\xi\right)c_{44}\right)\left(1+\alpha_1-s_2^2\alpha_2\right)+M\left(\xi\right)c_{44}s_2^2\alpha_3}{\xi c_{44}\left(s_1^2-s_2^2\right)\left(1+\alpha_1\right)\alpha_3} \tag{A.7}$$

$$B(\xi) = -\frac{\left(N(\xi)+M(\xi)c_{44}\right)\left(1+\alpha_1-s_1^2\alpha_2\right)+M(\xi)c_{44}s_1^2\alpha_3}{\xi c_{44}\left(s_1^2-s_2^2\right)\left(1+\alpha_1\right)\alpha_3} \tag{A.8}$$

Appendix B

The parameters in Eqs. (55) and (57) are:

$$m_k = \frac{c_{13}+c_{44}}{c_{33}s_k^2-c_{44}} \qquad (k=1,2) \tag{B.1}$$

$$\theta = \frac{1}{2\pi}\ln\left[\frac{\sqrt{\gamma_1'\gamma_2'}+\alpha}{\sqrt{\gamma_1'\gamma_2'}-\alpha}\right] \tag{B.2}$$

$$H = \frac{\left(\gamma_1'+\gamma_2'\right)c_{11}}{2\pi\left(c_{11}c_{33}-c_{13}^2\right)} \tag{B.3}$$

$$\alpha = \frac{\sqrt{c_{11}c_{33}}-c_{13}}{c_{11}\left(\gamma_1'+\gamma_2'\right)} \tag{B.4}$$

$$\gamma_k' = s_k^{-1} = \sqrt{\frac{m_k c_{33}}{m_k c_{44}+c_{13}+c_{44}}} \qquad (k=1,2) \tag{B.5}$$

Appendix C

Displacement and stress potential relations of the case of $s_1 = s_2$ are:

$$u_z(r,z) = \int_0^\infty \frac{\xi z \kappa_1 \left(N(\xi) + M(\xi) c_{44}\right) + M(\xi)\,\omega_1(\xi)\, c_{44} s_1 \alpha_3}{2c_{44} s_1 (1+\alpha_1)\,\alpha_3} \mathrm{e}^{-\xi s_1 z} J_0(\xi r)\,\mathrm{d}\xi \tag{C.1}$$

$$u_r(r,z) = \int_0^\infty \frac{\left(N(\xi) + M(\xi) c_{44}\right)\omega_2(\xi) + M(\xi)\, c_{44} s_1^2 \alpha_3 (1+\xi s_1 z)}{2c_{44} s_1 (1+\alpha_1)} \mathrm{e}^{-\xi s_1 z} J_1(\xi r)\,\mathrm{d}\xi \tag{C.2}$$

$$\sigma_{zz}(r,z) = -\int_0^\infty \frac{c_{13}\alpha_3 \Gamma_1(\xi) + c_{33}\Gamma_2(\xi)}{2c_{44} s_1 (1+\alpha_1)\,\alpha_3} \xi \mathrm{e}^{-\xi s_1 z}\mathrm{d}\xi \tag{C.3}$$

$$\sigma_{rz}(r,z) = -\int_0^\infty \frac{\xi z \kappa_1 N(\xi) + \alpha_3 s_1 \omega_3(\xi)\, N(\xi) + c_{44}\xi z \kappa_2 M(\xi)}{2 s_1 (1+\alpha_1)\,\alpha_3} \xi \mathrm{e}^{-\xi s_1 z} J_1(\xi r)\,\mathrm{d}\xi \tag{C.4}$$

where

$$\kappa_1 = \left(1 + \alpha_1 - s_1^2 \alpha_2\right)^2 \tag{C.5}$$

$$\kappa_2 = \left(1 + \alpha_1 + s_1^2 (\alpha_3 - \alpha_2)\right)^2 \tag{C.6}$$

$$\omega_1(\xi) = (2 + \xi s_1 z)(1+\alpha_1) - \xi s_1^3 \alpha_2 z \tag{C.7}$$

$$\omega_2(\xi) = (\xi s_1 z - 1)(1+\alpha_1) - s_1^2 \alpha_2 (1 + z \xi s_1) \tag{C.8}$$

$$\omega_3(\xi) = (\xi s_1 z - 2)(1+\alpha_1) - \xi s_1^3 \alpha_2 z \tag{C.9}$$

$$\omega_4(\xi) = 1 + \xi s_1 z \tag{C.10}$$

$$\omega_5(\xi) = 1 - \xi s_1 z \tag{C.11}$$

$$\Gamma_1(\xi) = \omega_5(\xi)\left(N(\xi) + M(\xi) c_{44}\right)\left((1+\alpha_1) + s_1^2\alpha_2\right) - \omega_4(\xi)\, M(\xi)\, c_{44}\alpha_3 s_1^2 \tag{C.12}$$

$$\Gamma_2(\xi) = -\omega_5(\xi)\,\kappa_1\left(N(\xi) + M(\xi) c_{44}\right) + M(\xi)\, c_{44}\alpha_3 s_1^2 \left(\omega_4(\xi)(1+\alpha_1) + \omega_5(\xi)\, s_1^2 \alpha_2\right) \tag{C.13}$$

Table captions

Table 1. Properties of synthetic materials.

Figure captions

Figure 1. Axial translation of a rigid disc inclusion embedded in a penny-shaped crack.

Figure 2. Axial translation of a rigid disc inclusion located at a cracked plane: Limiting cases. (a) An intact full-space medium; (b) Two half-space regions; (c) Direct loading of a penny-shaped crack

Figure 3. Axial stiffness for synthetic materials. (a) The effect of E'; (b) The effect of G' and (c) The effects of E and G

Figure 4. Normalized mode II stress intensity factor for synthetic materials. (a) The effect of E'; (b) The effect of G' and (c) The effects of E and G

Table 1. Properties of synthetic materials.

Material	E	E'	G	G'	E/E'	G/G'	ν, ν'	c_{11}	c_{12}	c_{13}	c_{33}	c_{44}	c_{66}
1[a]	5	5	2	2	1	1	0.25	6	2	2	6	2	2
2[b]	5	10	2	2	0.5	1	0.25	5.6	1.6	1.8	10.9	2	2
3[b]	5	25	2	2	0.2	1	0.25	5.4	1.4	1.7	25.9	2	2
4[b]	5	5	2	1	1	2	0.25	6	2	2	6	1	2
5[b]	5	5	2	0.67	1	3	0.25	6	2	2	6	0.67	2
6[b]	5	5	2	0.4	1	5	0.25	6	2	2	6	0.4	2
7[b]	10	5	4	2	2	2	0.25	14	6	5	7.5	2	4
8[b]	15	5	6	2	3	3	0.25	26	14	10	10	2	6
9[b]	25	5	10	2	5	5	0.25	110	90	50	30	2	10

[a]Isotropic [b]Transversely isotropic

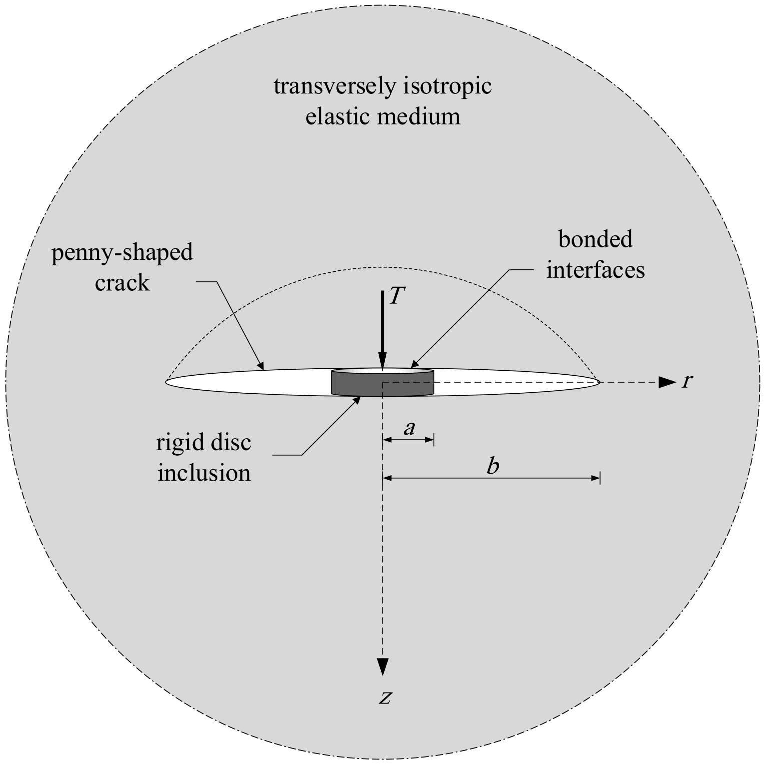

Figure 1. Axial translation of a rigid disc inclusion embedded in a penny-shaped crack.

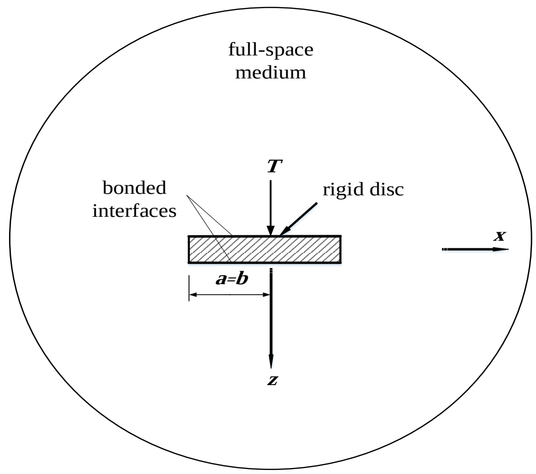

(a) An intact full-space medium

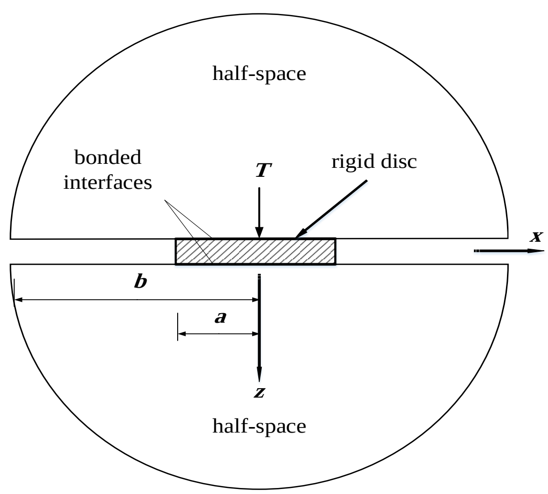

(b) Two half-space regions

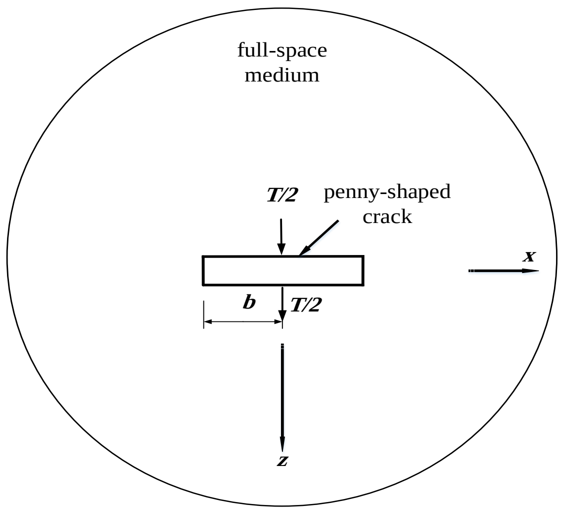

(c) Direct loading of a penny-shaped crack

Figure 2. Axial translation of a rigid disc inclusion located at a cracked plane: Limiting cases.

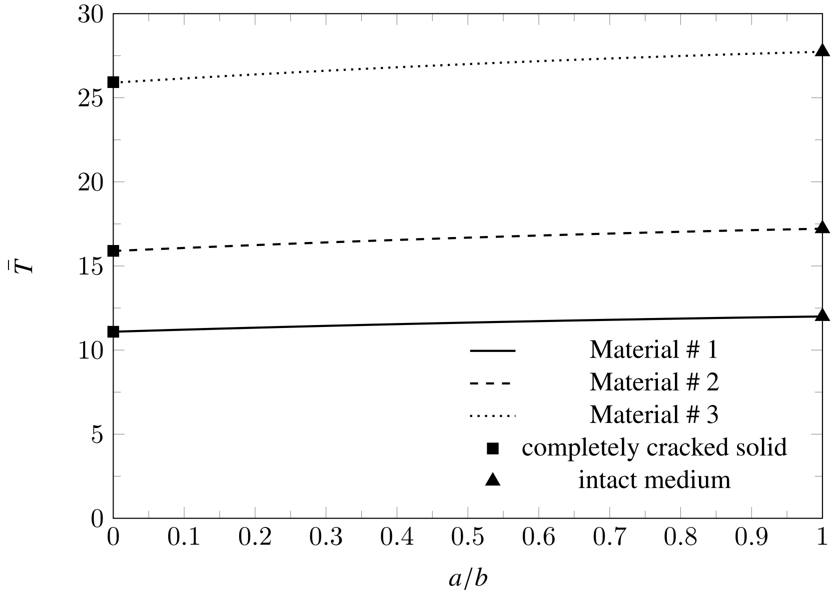

(a) The effect of E'

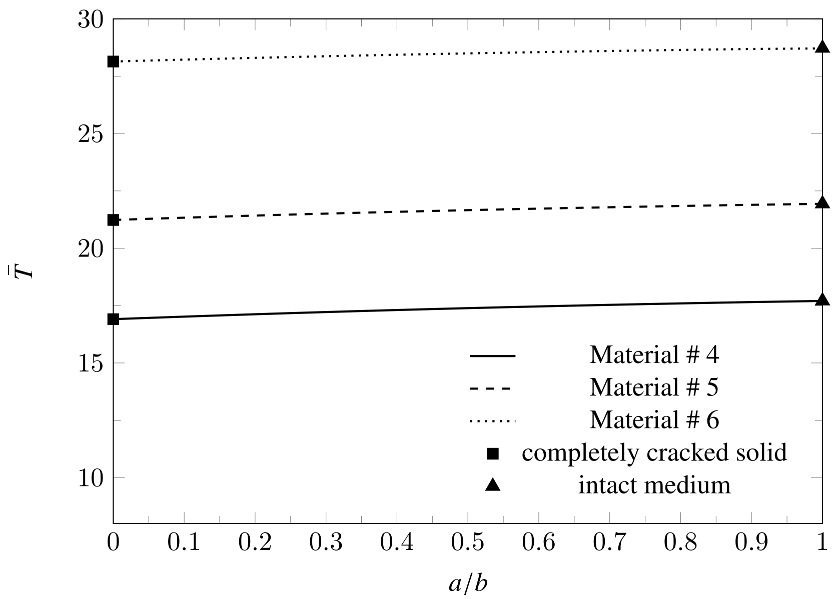

(b) The effect of G'

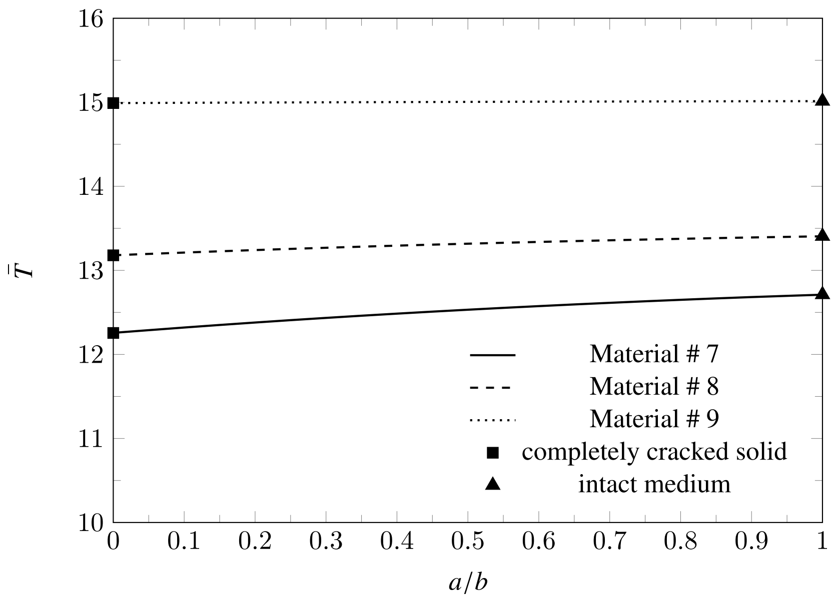

(c) The effects of E and G

Figure 3. Axial stiffness for synthetic materials.

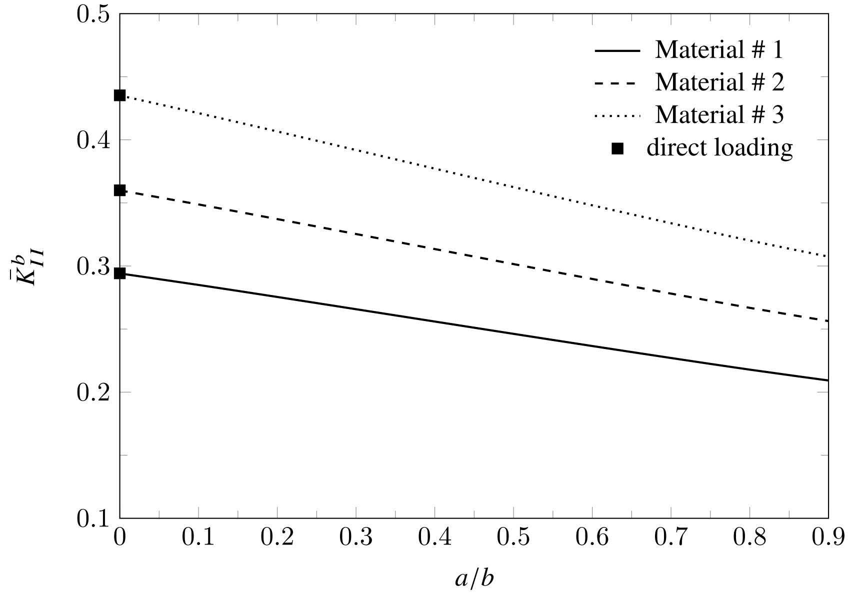

(a) The effect of E'

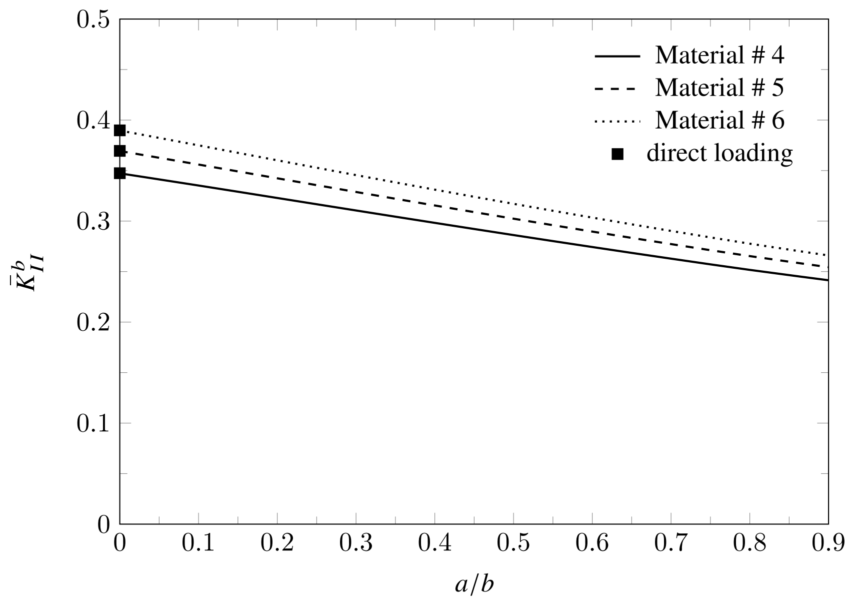

(b) The effect of G'

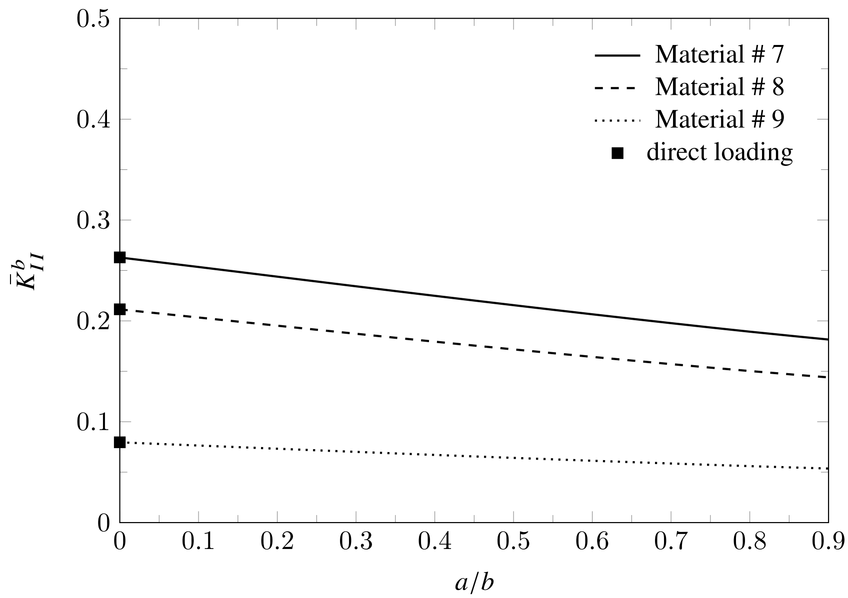

(c) The effects of E and G

Figure 4. Normalized mode II stress intensity factor for synthetic materials.